Kidney International, Vol. 67 (2005), pp. 1275–1285

HORMONES – CYTOKINES – SIGNALING

Differential proteomic analysis of proteins induced by glucocorticoids in cultured murine podocytes

RICHARD F. RANSOM, VIRGINIA VEGA-WARNER, WILLIAM E. SMOYER, and JON KLEIN

Pediatric Nephrology Division, University of Michigan, Ann Arbor, Michigan; Department of Medicine and Department of Biochemistry and Molecular Biology, University of Louisville, Louisville, Kentucky

Differential proteomic analysis of proteins induced by glucocorticoids in cultured murine podocytes.

Background. The glomerular podocyte is the kidney cell most affected during the development of nephrotic syndrome, and mutations in podocyte proteins are responsible for a variety of inherited forms of nephrotic syndrome. Although glucocorticoids are a primary treatment for nephrotic syndrome, neither their target cell nor mechanism of action are known. In order to describe the proteome of the podocyte, and to identify podocyte proteins whose expression is altered by glucocorticoids, we performed a differential proteomic analysis of control and dexamethasone-treated cultured murine podocytes.

Methods. Podocyte proteins were separated by two-dimensional-polyacrylamide gel electrophoresis (PAGE) and identified by matrix-assisted laser desorption time-of-flight (MALDI-TOF) mass spectrometry and peptide fingerprinting. Comparisons of stained two-dimensional-PAGE separations were used to identify proteins whose expression was altered by treatment with the glucocorticoid dexamethasone, and these results were confirmed by quantitative Western blotting.

Results. A total of 106 protein spots yielded MALDI-TOF results, and 92 were identified by protein fingerprinting. Of the 88 unique proteins and four protein isoforms identified, six proteins were found whose expression was altered by dexamethasone. The proteome of cultured murine podocytes is particularly rich in actin cytoskeletal proteins and proteins involved in responses to cellular stress. The change in expression of three proteins [ciliary neurotrophic factor (CNTF), αB-crystallin, and heat shock protein 27 (hsp27)] was confirmed by quantitative Western blotting.

Conclusion. Three proteins with known roles in protecting cells from injury were up-regulated by dexamethasone, demonstrating that glucocorticoids exert a direct effect on cultured podocytes resulting in changes in the expression of proteins with potential relevance to the therapeutic action of glucocorticoids in diseases such as nephrotic syndrome.

Key words: ciliary neurotrophic factor, heat shock protein, dexamethasone, nephrotic syndrome, actin cytoskeleton.

Received for publication March 12, 2004
and in revised form July 1, 2004
Accepted for publication October 12, 2004

The glomerular podocyte is increasingly recognized as a primary determinant of focal segmental glomerular sclerosis leading to chronic kidney disease [1, 2], and recent discoveries have highlighted the importance of podocyte proteins in maintaining the glomerular filtration barrier in both health and disease [3]. The podocyte cell body floats in the urinary space of the glomerulus, and its primary processes extend to the glomerular capillary, where secondary and tertiary "foot" processes interdigitate and attach to the underlying glomerular basement membrane (GBM). Specialized adherens junctions called slit diaphragms span the filtration slits between foot processes. The slit diaphragms, together with the GBM and fenestrated endothelium of the glomerular capillary, form the kidney's filtration barrier. Because the podocyte is encapsulated within the glomerulus and attached through its extensive network of foot processes to the GBM, isolation of a significant number of podocytes for primary culture or biochemical analyses is problematic. In order to overcome this difficulty, a number of researchers have isolated cell lines from glomerular outgrowths [4–7], including a conditionally-immortalized podocyte cell line expressing a temperature sensitive form of the SV40 T-antigen was derived from the Immortomouse [8]. These cells can be differentiated to become nonproliferative, arborized cells expressing at least a subset of the proteins characteristic of podocytes in vivo [9]. These murine podocytes, along with a recently-described line of conditionally immortalized podocytes of human origin [7], represent the best currently available model system for analysis of the biochemistry of the podocyte.

Nephrotic syndrome is common in adults and is among the most common kidney diseases in children [10]. During development of nephrotic syndrome, several morphologic changes occur in glomerular podocytes, including retraction and effacement of the podocyte foot processes, formation of occluding junctions with displacement of slit diaphragms, and, in severe cases or specific areas, detachment of the podocyte from the GBM [11–15]. Foot process effacement correlates closely with the development

of proteinuria [12, 14, 16], and is the characteristic ultrastructural finding for nephrotic syndrome.

The most commonly used treatment for nephrotic syndrome is oral glucocorticoids, although despite their frequent use, neither the target cell nor the mechanism of action of glucocorticoids in inducing remission in patients with nephrotic syndrome has been identified. Due to the absence of inflammatory cells in the glomeruli of patients with typical idiopathic nephrotic syndrome [17], soluble factors, presumably secreted by circulating lymphocytes [18, 19], have long been implicated as causative agents in this disease. Although extensively studied for more than 25 years, no consistent abnormalities in either secreted cytokines, or in the number of total or subsets of T lymphocytes, have been identified to date (reviewed in [20]). The known anti-inflammatory and immunosuppressive activities of glucocorticoids have historically been taken as indirect evidence suggesting that their mechanism of action in nephrotic syndrome involves inhibition of release of soluble mediators by T lymphocytes [21]. Recently, however, glomerular podocytes have been shown to contain the glucocorticoid receptor, and the receptor has been shown to translocate to the nucleus of podocytes upon dexamethasone treatment [22], demonstrating that podocytes are capable of responding to glucocorticoids. We have recently discovered that treatment of cultured podocytes with dexamethasone both protects from and ameliorates injury caused by puromycin aminonucleoside (PAN), a compound used to induce experimental nephrotic syndrome in animals. In addition, dexamethasone enhances the stability of actin filaments against subsequent disruption by cytochalasin D or latrunculin A [23]. These findings provide strong evidence suggesting that glucocorticoids may in fact exert at least part of their therapeutic action in nephrotic syndrome by acting directly on podocytes rather than via their effects on lymphocytes.

Proteomic analyses are an increasingly common technique for characterizing the proteins expressed in normal organs, tissues, and cells, and for examining the coordinated changes of proteins in response to various stimuli. Proteomic analyses permit the identification of a large number of proteins expressed by a particular cell or tissue, typically by separation of proteins by two-dimensional polyacrylamide gel electrophoresis (PAGE) or microcapillary liquid chromatography, followed by identification using mass spectrometry. This analysis permits characterization of protein modifications and of translational regulation that is not available through genomic measurements of changes in mRNA expression. We hypothesized that a proteomic analysis of cultured murine podocytes would reveal important clues concerning the nature of these unique cells, and that a differential proteomic analysis of the proteins altered by dexamethasone treatment would identify proteins that may be responsible for the observed protective and ameliorative effects of dexamethasone in podocytes. The present study was performed to create a proteome map of the proteins expressed in differentiated cultured murine podocytes [8], and to discover and identify proteins whose expression in these cells is altered by dexamethasone 3 days after treatment, a time point when podocyte actin filaments were most resistant to disruption by cytochalasin D and latrunculin A [23].

METHODS

Cell culture

Murine podocytes derived from the Immortomouse [8] were cultured and differentiated as previously described [24]. Briefly, cells of passage number ≤ 10 were grown in RPMI 1640 medium containing penicillin and streptomycin antibiotics, 10% fetal bovine serum (FBS) (Gibco Invitrogen, Carlsbad, CA, USA), and 10 U/mL of interferon-γ (INF-γ) at 33°C, and differentiated in the same medium without INF-γ at 37°C (Sigma Chemical Co., St. Louis, MO, USA). Cells used in these studies were seeded at 3.0×10^5 cells per 75 cm^2 culture flask or 3.0×10^4 per well of a 6-well tissue culture plate (Greiner Bio-One, Longwood, FL, USA) and differentiated for 10 to 14 days with medium changes every 4 to 5 days. Medium was changed 12 hours prior to dexamethasone treatment. Treatment consisted of a medium change to medium containing vehicle or 1 μmol/L water-soluble dexamethasone (Sigma Chemical Co.), followed 30 minutes later by another change to medium alone. Treated cells were cultured for a further 12 hours to 7 days, and for proteomic analysis were collected 3 days after dexamethasone treatment by brief trypsin digestion followed by centrifugation at $1000 \times g$ for 3 minutes, and were then washed once with warm phosphate-buffered saline (PBS) and recentrifuged.

Phase contrast and fluorescence microscopy

Cultured podocytes differentiated on glass coverslips were washed in warm PBS, fixed in 3.7% paraformaldehyde (Electron Microscopy Sciences, Hatfield, PA, USA) in PBS for 20 minutes, and lysed by addition of an equal volume of 0.25% Triton X-100 (Electron Microscopy Sciences) in PBS and incubation for a further 5 minutes. Lysed podocytes were incubated for 20 minutes in 0.05% Tween-20 in PBS (T-PBS) containing 66 nmol/L Oregon Green 488™ phalloidin (Molecular Probes, Eugene, OR, USA) for phase contrast and phalloidin fluorescence microscopy. In order to visualize synaptopodin, lysed podocytes were incubated for 1 hour in 5% heat-denatured horse serum in T-PBS to block nonspecific protein binding sites, labeled with antisynaptopodin antibody (mouse monoclonal antisynaptopodin clone G1D4) (Research Diagnostics, Flanders, NJ, USA) diluted 1:2

in 5% horse serum in T-PBS for 1 hour, washed thoroughly in T-PBS, and incubated for 1 hour with Texas Red–conjugated goat antimouse antibody (Jackson Immuno Research Laboratories, West Grove, PA, USA) diluted 1:100 in 5% horse serum in T-PBS. After washing in T-PBS, all specimens were mounted in Prolong Anti-Fade™ mounting reagent (Molecular Probes) and micrographs collected using OpenLab software (Improvision, Lexington, MA, USA) controlling a Retiga 1300 120-bit grayscale charged coupling device (CCD) camera (QImaging, Burnaby BC, Canada) collecting images from a Leica DM IRE2 fluorescence microscope (Leica Microsystems, Bannockburn, IL, USA).

Western blotting

Podocytes were cultured in 6-well plates and treated ($N = 4$ samples/treatment) for various times with either dexamethasone or vehicle alone. They were washed with warm PBS and proteins were extracted into 150 μL of sodium dodecyl sulfate (SDS)-PAGE sample buffer (62.5 mmol/L Tris-Cl, pH 6.8, 10% glycerol, and 2% SDS) with gentle rocking for 10 minutes at room temperature. Extracts were collected, centrifuged at 10,000 × *g* for 15 minutes, and an aliquot removed for protein assay by BCA microassay (Pierce, Rockford, IL, USA). 2-Mercaptoethanol containing 0.2% bromophenol blue was added to samples to a final concentration of 5%, and samples were heated to 100°C for 4 minutes and recentrifuged. Aliquots of sample supernatants containing 30 μg of total protein, and serial dilutions of standard proteins [αB-crystallin and murine heat shock protein 27 (hsp27) (Stressgen, Victoria, BC, Canada) and ciliary neurotrophic factor (CNTF) (Santa Cruz Biotechnology, Santa Cruz, CA, USA)] dissolved in sample buffer were loaded onto 12% discontinuous polyacrylamide gels, separated by electrophoresis, and transferred to polyvinlydine difluoride (PVDF) membranes by immersion blotting. Membranes were washed in PBS containing PBS-T, nonspecific protein binding sites were blocked by incubation for 1 hour in 5% nonfat dry milk (Bio-Rad, Hercules, CA, USA) in PBS-T, washed three times in PBS-T, and incubated for 2 hours in primary antibody solutions made in 5% bovine serum albumin (BSA) (Fraction V) (Sigma Chemical Co.) in PBS-T. Antibodies specific for murine hsp27 and aB-crystallin (Stressgen) were used at 1:5000 dilution, for CNTF (Santa Cruz Biotechnology) at 1:2000 dilution, and for annexin V (Santa Cruz Biotechnology) at 1:1000 dilution. After three washes, membranes were incubated with horseradish peroxidase-conjugated antirabbit or mouse IgG secondary antibodies (Jackson Immunochemicals, West Grove, PA, USA) diluted 1:10,000 in 5% nonfat dry milk in PBS-T for 1 hour. Membranes were washed again, and antibody binding was visualized using an enhanced chemiluminescence reagent (SuperSignal West Pico substrate) (Pierce) as detected by a CCD camera imaging system (ChemiDoc) (Bio-Rad). The integrated signal density from antibody staining in digital images of Western blots was measured using Quantity One software (Bio-Rad). Amounts of αB-crystallin, hsp27, and CNTF proteins were derived from the linear portion of standard curves of the integrated density of standard protein signals vs. the quantity of standard protein loaded. Percent of control values described in the text are the percentage of the average amount of each specific protein in dexamethasone-treated samples compared to the average amount of that protein in time-matched controls.

Sample preparation for two-dimensional-PAGE

Cell pellets from 75 cm^2 flasks were suspended in sample buffer consisting of 7 mol/L urea, 2 mil/L thiourea (Fisher, Fair Lawn, NJ, USA), 60 mmol/L dithiotreitol (DTT), 4% CHAPS (Sigma Chemical Co.), and 1.8% (solids) 3/10 ampholytes (Bio-Rad). Suspensions were agitated on a vortex mixer for 1 hour and centrifuged at 16,000 × *g* for 10 minutes, and quantities of the supernatant containing equal amounts of total protein were loaded onto the first-dimension isoelectric focusing (IEF) gel for proteomic analysis. The protein concentration in supernatants was measured by spectrophotometry using HP 8453 ultraviolet-visible system (Hewlett-Packard Company, Palo Alto, CA, USA) and Bio-Rad RCDC Protein Assay (Bio-Rad).

First dimension of two-dimensional PAGE

An immobilized pH gradient (IPG) IEF gel (pH 3 to 10) (Genomic Solutions Inc., Ann Arbor, MI, USA) was used for first-dimensional isoelectric focusing using 100 mmol/L sodium hydroxide as the cathode buffer, and 10 mmol/L phosphoric acid as the anode buffer. The protein samples (100 μg total protein) were loaded onto the IEF gels with the rehydration buffer and were focused for 17 hours and 30 minutes to reach 18000 volt-hours.

Second dimension of two-dimensional PAGE

The IPG first-dimension strips were incubated in premixed Tris/acetate equilibration buffer with 0.01% bromophenol blue and 50 mmol/L DTT for 2 minutes before loading onto precast 10% homogeneous, 22 × 22 cm, slab gels (Genomic Solutions). Upper running buffer consisted of 0.2 mol/L Tris base, 0.2 mol/L tricine, and 0.4% SDS and lower running buffer was 0.625 mol/L Tris/acetate. The system was run with maximum of 500 volts and 20,000 milliwatts per gel.

SYPRO Ruby™ staining and visualization

The slab gels were fixed in 10% methanol and 7% acetic acid for 30 minutes. The fixation solution was removed and gels were incubated in 500 mL of SYPRO Ruby™

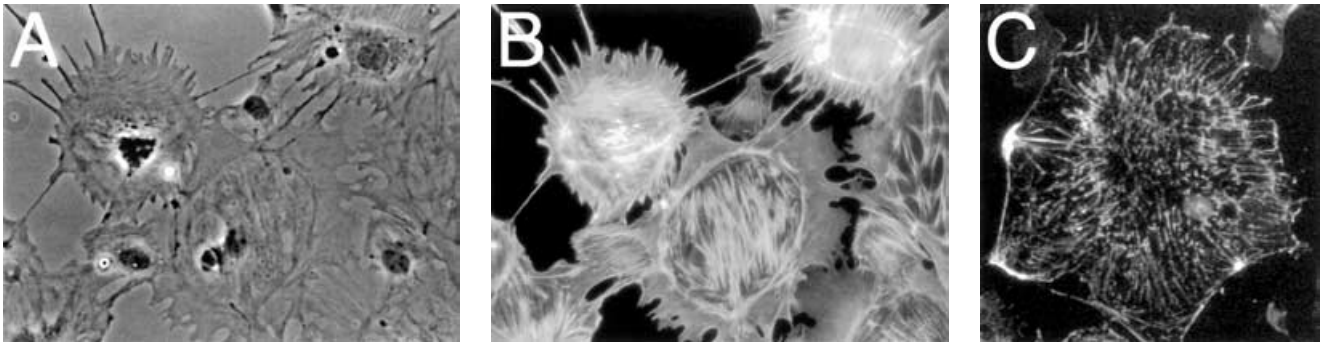

Fig. 1. Phase contrast and fluorescence micrographs of differentiated podocytes labeled to visualize filamentous actin and synaptopodin. Cultured podocytes were induced to differentiate, fixed, viewed by phase contrast microscopy (*A*), or labeled with either Oregon Green 488™ phalloidin (*B*) or antisynaptopodin antibody and an appropriate Texas Red-conjugated secondary antibody (*C*) and viewed under fluorescence illumination. The micrographs in (A and B) are of the same field (white bar at lower right = 40 μm).

gel stain (Bio-Rad) with gentle, continuous rocking for 18 hours at room temperature. A high-resolution 12-bit camera with ultraviolet light box system (Genomic Solutions) was used to visualize the gel images. Gels were exposed to ultraviolet light for an optimal time of 3 seconds.

Quantitative analysis of protein expression

Investigator HT analyzer (Genomic Solutions) software was used for matching and analysis of the spots on the gels. Individual spots were matched across gels initially using automated spot recognition algorithms and then were confirmed by hand. Spot intensities were first normalized to total gel fluorescence as an initial adjustment for intergel background variability. A separate analysis of each spot's fluorescence intensity was then performed in each gel with additional correction for local background variability. The average gel was constructed as a represented gel for each experimental group ($N = 7$ in each group). Average mode of background subtraction was used to normalize the intensity volume that represents the amount of protein per spot. The average gel was then used for determination of the presence of and difference of protein expression between each group.

In-gel tryptic digestion, matrix-assisted laser desorption time-of-flight (MALDI-TOF) mass spectrometry, and peptide mass fingerprinting

In-gel tryptic digestion and MALDI-TOF mass spectrometry were performed using techniques described previously [25]. Protein identification of peptide fragments was performed by using the "Profound" search engine (*http://129.85.19.192/profound_bin/WebProFound.exe*) based on the entire NCBI protein database using the assumption that peptides are monoisotopic, oxidized at methionine residues, and carboxamidomethylated at cysteine residues. Up to one missed trypsin cleavage was allowed, although most matches did not contain any missed cleavages. Mass tolerance of 150 ppm was the window of error allowed for matching the peptide mass values. Z scores were estimated by comparison of search results against estimated random match population and were the distances to the population mean in units of standard deviation. Scores greater than 1.65 were considered statistically significant ($P < 0.05$). Identities of protein spots that did not reach this significant level were not reported.

Statistical analyses

Both unpaired Student *t* test and the exact mode of the Mann-Whitney test (SigmaPlot) (SPSS, Inc., Chicago, IL, USA) were used for comparisons of the differences between two groups ($N = 7$ for each group) of staining intensities in analyses of two-dimensional-PAGE separations. *P* values less than 0.05 were considered statistically significant. This significance level is based on the exact distribution of a test statistic that is more accurate than using asymptotic significance values when the sample size is small. Only the significances that were in agreement between the Student *t* test and the Mann-Whitney test were reported. Data are reported as mean ± SEM.

The unpaired Student *t* test was used for comparison of protein quantities derived from standard curves of luminescence intensities on Western blots. Data were reported as mean ± SEM, with P values < 0.05 considered significant.

RESULTS

Cultured podocyte morphology and synaptopodin labeling

The cultured podocyte used in this study displayed an arborized morphology with long, well-developed cell processes (Fig. 1A) containing actin filaments (Fig. 1B). These cells also stained for synapotopodin in a

filamentous pattern characteristic of this podocyte-specific actin-associated protein (Fig. 1C).

Proteomic analysis of cultured podocytes

Protein spots were isolated from two-dimensional-PAGE separations of extracts of differentiated, cultured murine podocytes and subjected to MALDI-TOF mass spectrometry and protein fingerprinting. Of 106 protein spots yielding MALDI-TOF results, 92 were identified by a search of the NCBI protein database using the Profound search engine. Of the identified proteins (Table 1), 88 were unique proteins and four were protein isoforms of one of the identified proteins (moesin, nonmuscle caldesmon, vimentin, and heterogeneous nuclear riboprotein K). Identified proteins were of the expected pI and molecular weight in two-dimensional-PAGE separations.

The proteins identified in cultured podocytes were organized into categories (Table 1) based on functional information in their PubMed and SwissProt protein database entries and on other published reports. As expected, a number of metabolic enzymes and enzymes involved in amino acid synthesis and other basic cellular functions were identified. Podocytes also expressed several members of classes of proteins important for response to cellular stress, including antioxidant enzymes, heat shock proteins, and chaperonins. Members of several classes of cell signaling proteins, including phosphatases, guanosine diphosphate (GDP) dissociation inhibitors, transcription factors, and the 14–3-3 zeta scaffolding protein were identified. The largest class of proteins found in podocytes was cytoskeletal proteins, and, in particular, actin cytoskeletal proteins and proteins primarily known for their association with the actin cytoskeleton. Several classes of proteins were also found and grouped by their association with subcellular organelles such as the endoplasmic reticulum, mitochondria, and the plasma membrane (e.g., annexins). Finally, several proteosome proteins, serine protease inhibitors, an intracellular chloride channel, and a protein previously described as a neuronal cytokine (CNTF) were identified.

Comparative proteomic analysis of dexamethasone-treated podocytes

Proteins were extracted from cultured murine podocytes 3 days after a 30-minute treatment of seven cultures each with vehicle or with 1 μmol/L dexamethasone, and extracted proteins were separated by two-dimensional-PAGE. The results of analyses of stained two-dimensional-PAGE separations (representative stained separations of extracts from vehicle and dexamethasone-treated podocytes are shown in Fig. 2) were used to determine differences in protein expression between vehicle- and dexamethasone-treated podocytes.

These analyses revealed six proteins whose expression was significantly altered 3 days after dexamethasone treatment when compared with extracts from cells treated with vehicle alone (Table 2). The expression of five of these proteins (purine nucleotide phosphorylase, annexin 5, CNTF, αB-crystallin, and gelsolin) was significantly increased by dexamethasone, and only the expression of the lysosomal adenosine triphosphatase (ATPase) proton pump was significantly reduced after dexamethasone treatment.

Confirmation of proteomic results by quantitative Western blotting

The increases in the amounts of CNTF and αB-crystallin proteins at 3 days observed in our proteomic analysis were confirmed by a Western blot analysis using appropriate antibodies against these proteins. The magnitudes of the increases in CNTF and αB-crystallin protein 3 days after dexamethasone treatment derived from measurements of chemiluminescence compared to standard proteins (250% and 301% of time-matched controls, respectively) were greater than the values obtained by comparison of stained gels in the proteomic analyses (197% and 165% of time-matched controls, respectively). In addition, the amount of CNTF and αB-crystallin was higher in dexamethasone-treated podocytes than in time-matched controls as early as 1 day after dexamethasone treatment and remained elevated for at least 7 days (Fig. 3). The largest amount of these proteins was found in podocytes at 7 days after dexamethasone treatment, with 14.5 ± 1.5 ng of CNTF per 1000 cells (277% of time-matched controls) and 1.27 ± 0.1 ng of αB-crystallin per 1000 cells (463% of time-matched controls). We also noted increases in the amount of hsp27 (Fig. 3), a small heat shock protein closely related to αB-crystallin, that were comparable in magnitude (425% of time-matched controls at 1 day after dexamethasone treatment) but reached maximal levels earlier (1 day after treatment) than dexamethasone-induced increases in αB-crystallin expression. We were unable to reproducibly confirm changes in the amount of annexin 5 induced by dexamethasone by quantitative Western blotting. We did not measure changes in the amounts of purine nucleoside phosphorylase, lysosomal ATPase, or gelsolin in extracts of podocytes.

DISCUSSION

This study was designed to identify proteins of the proteome of cultured differentiated murine podocytes, and to discover and identify podocyte proteins whose expression was altered by a glucocorticoid treatment previously shown to protect these cells from injury and direct cytoskeletal disruption. We successfully identified a total of 92 protein spots representing 88 unique proteins,

Table 1. Proteins identified in cultured murine podocytes by proteomic analysis

Protein	Spot number	GI number	Molecular weight	pI
Metabolic enzymes				
Aldolase 1, alpha isoform	88	6671539	39800	8.31
Enolase 1, alpha non-neuron	65	13637776	47500	6.37
Lactate dehydrogenase	57	65923	36800	7.62
Lactate dehydrogenase 2, B chain	4	6678674	36834	5.7
Malate dehydrogenase, soluble	19	31982178	36600	6.16
3-Phosphoglycerate dehydrogenase	29	13928850	57200	6.28
Phosphoglycerate kinase	87	129903	44900	8.0
Phosphoglycerate mutase type B subunit	6	8248819	28930	6.7
Pyruvate kinase 3; M2 isozyme	16	1363219	58400	7.58
Transketolase	84	12018252	71940	7.54
Antioxidant enzymes				
Cu/Zn-superoxide dismutase	89	201006	16100	6.23
Glutathione-S-transferase, mu 1	77a	6754084	26100	7.71
Peroxiredoxin 1	80	547923	22500	8.26
Peroxiredoxin 2 (type II peroxiredoxin-1)	34	3603241	22000	5.2
Peroxiredoxin 6 (1-Cys peroxiredoxin protein)	39	4139186	25000	5.98
Other enzymes				
Aldose reductase	58	1351911	34700	7.04
ATPase, lysosomal H+ transport, subunit D, isoform 2	100	31981304	56900	5.6
Cytosolic nonspecific dipeptidase	17	31981273	53162	5.43
Esterase 10, D	20	13937355	37800	6.7
Glucose-regulated protein, 58 kD (phospholipase C, alpha)	13	20911547	57099	5.88
Glutamate dehydrogenase	28	6680027	61700	8.05
Ornithine aminotransferase	61	8393866	48700	6.19
Peptidylprolyl isomerase A; cyclophilin A	43	6679439	18131	7.74
Purine-nucleoside phopshorylase	10	7305395	32527	5.78
Thioether S-methyltransferase	5	6678281	30068	6
Ubiquinol-cytochrome c reductase core protein 1	95	13384794	53400	5.8
UMP-CMP kinase (cytidylate kinase)	91	23821758	22400	5.68
Phosphatases				
Protein phosphatase 1 alpha	97	13994195	38300	5.9
Protein phosphatase 1 delta	98	227436	38000	5.8
Phosphoprotein phosphatase	66	1663530	54700	6.23
GDP dissociation inhibitors				
Rab GDP dissociation inhibitor alpha	102	21903424	51000	4.96
GDP dissociation inhibitor 3	9	6679987	51000	5.93
Rho GDP dissociation inhibitor 1	2	31982030	23464	5.12
Nuclear proteins				
Par-4 (PRKC, apoptosis response protein)	30	20865316	36000	5.74
Heterogeneous nuclear ribonucleoprotein K	69, 70	13384620	51300	5.19
Bat1 nuclear RNA helicase	96	19773876	49400	5.43
Other regulatory proteins				
14–3-3 Zeta protein	82	7435027	27900	4.72
Actin cytoskeletal and binding proteins				
Actin-related protein (Arp) 3	8	12835802	47743	5.54
Ezrin (villin 2)	93	32363497	69500	5.9
F-actin capping protein alpha-1 subunit	103	1345694	33000	5.34
F-actin capping protein alpha-2 subunit	106	6671672	33500	5.57
F-actin capping protein beta-subunit (Cap Z)	36	34223730	31000	5.5
Nonmuscle caldesmon	45, 46	2498205	65000	6.34
Gelsolin	94	18606238	81000	5.5
LIM and SH3 protein 1 (Lasp-1)	41	6754508	30300	6.61
Moesin	27	13540689	68000	6.2
Moesin	92	462608	67800	6.22
Myosin regulatory light chain 2-a, smooth muscle isoform	52	127170	19900	4.78
Septin 6	15	20178348	50000	6.36
Transgelin 2	81	9910901	22500	8.39
Tropomyosin, alpha isoform, nonmuscle	51	207351	32700	4.76
Tropomyosin, alpha isoform	33	14134104	32773	4.7
Tropomyosin 4	23	6981672	28564	4.66
Tropomyosin 5	83	111212	29200	4.75
Vimentin	49, 50	2078001	53700	4.96
Other cytoskeletal proteins				
Laminin receptor 1	31	31560560	33000	4.8
Tubulin alpha 1	25	33440506	50100	4.94
Calcium-dependent protease, small subunit	35	18202239	28500	5.41
Translationally controlled tumor protein 1	44	6678437	19600	4.8
Collapsing response mediator protein 2 (CRMP-2)	14	40254595	62531	5.95

Table 1. (Continued).

Protein	Spot number	GI number	Molecular weight	pI
Annexins				
Annexin I	11	6754570	38952	6.56
Annexin II	7	6996913	39000	7.55
Annexin III	3	7304887	36533	5.33
Annexin IV	21	2492905	36200	5.43
Annexin V	24	6753060	35787	4.83
Annexin VII	60	584761	50200	5.91
Heat shock proteins				
Alpha B-crystallin	42	6753530	20000	6.76
Hsp8, Hsp cognate 70	1	31981690	71021	5.37
Hsp60 protein	12	1334284	58061	5.35
Stress-70 protein, mitochondrial precursor (Mortalin)	67	1346171	74000	5.72
Chaperonins				
T complex polypeptide (TCP) 1	72	201725	60000	5.82
TCP-1 beta subunit	63	5295927	57800	5.97
TCP-1 theta subunit	71	1174621	60000	5.44
Chaperonin subunit 5 (epsilon)	47	6671702	60000	5.7
Proteosome proteins/protease inhibitors				
Proteasome 28 subunit, alpha	37	6755212	28800	5.73
Proteasome subunit, alpha type 1	38	9910833	29800	6
Proteasome subunit, beta type, 4	90	3914439	29200	5.47
Serine protease inhibitor 3	105	6678097	42900	5.53
Phosphatidylethanolamine binding protein	54	9256572	21000	5.2
Endoplasmic reticulum proteins				
Protein disulfide isomerase precursor (PDI)	68	129729	57500	4.79
Calreticulin	32	6680836	48100	4.33
78 kD glucose-related protein precursor (GRP78, Bip)	101	2506545	72500	5.07
Protein disulfide isomerase A3 precursor (GRP58, HIP-70)	104	1352384	57000	5.9
Mitochondrial proteins				
Chlorine intracellular channel 4, mitochondrial (mtCLIC/CLIC4)	55	7304963	29000	5.44
ATP synthase, H+ transporting, mitochondrial F1 complex	85	6680748	59800	9.2
Prohibitin	56	6679299	29800	5.57
Other proteins				
Chloride intracellular channel 1	22a	15617203	27338	5.09
Ciliary neurotrophic factor (CNTF)	40	16507247	22600	6.05

GI, GenInfo identifier; pI, isoelectric pH value.

and determined that the expression of six of these proteins was altered by treatment with dexamethasone. In addition to identifying two glucocorticoid-up-regulated proteins with known roles in cell survival (CNTF and αB-crystallin), a third up-regulated protein (hsp27) was identified by Western blotting due to its high homology to αB-crystallin.

We present for the first time, to our knowledge, a proteomic analysis of a glomerular cell type (podocyte), and a differential analysis of changes in protein expression in any cell type in response to glucocorticoids. A limited number of renal proteomic analyses have been performed to date, including proteomic profiles of urine proteins [26–29], renal cancer cells [30, 31], isolated proximal tubules [32], and kidney tissue [29, 33]. The only analysis we are aware of on the effect of steroids on the mammalian proteome is a study describing a genomic and proteomic analysis of prostate cancer cells in response to dihydroxytestosterone [34].

The proteome of differentiated, cultured murine podocytes is particularly rich in actin cytoskeletal proteins, annexins, and stress-associated proteins such as heat shock proteins and antioxidant enzymes (Table 1). Only a limited subset of the proteins identified in cultured podocytes were also found in other proteomic analyses of the kidney, the majority of overlap consisting of cytoskeletal proteins [35, 36], as well as hsp60, αB-crystallin, and chloride intracellular channel 1 [33]. The commonality of cytoskeletal proteins between podocytes and kidney proteomes may simply be a function of their ubiquitous expression and relatively high abundance in eukaryotic cells. It is, however, difficult to draw any conclusions from the relative paucity of proteins common to the podocyte proteome described in this analysis and other currently available kidney proteomes analyses, primarily because the published renal proteomes consist only of proteins differentially expressed in response to some stimulus [36] or common in both cortical and medullary tissues [33, 37]. Proteomic analyses of renal cell carcinomas [30, 31], cultured fibroblasts [38], umbilical vein endothelial cells [39], and, in particular, cultured, differentiated mammary cells [40] contained a larger and more diverse subset of proteins in common with cultured, differentiated podocytes. The greater overlap between known proteomes of cultured cells than between cultured podocytes and whole kidney is not particularly noteworthy, particularly since the analyses of renal tissues were restricted to a small subset of identified proteins. The major species present in

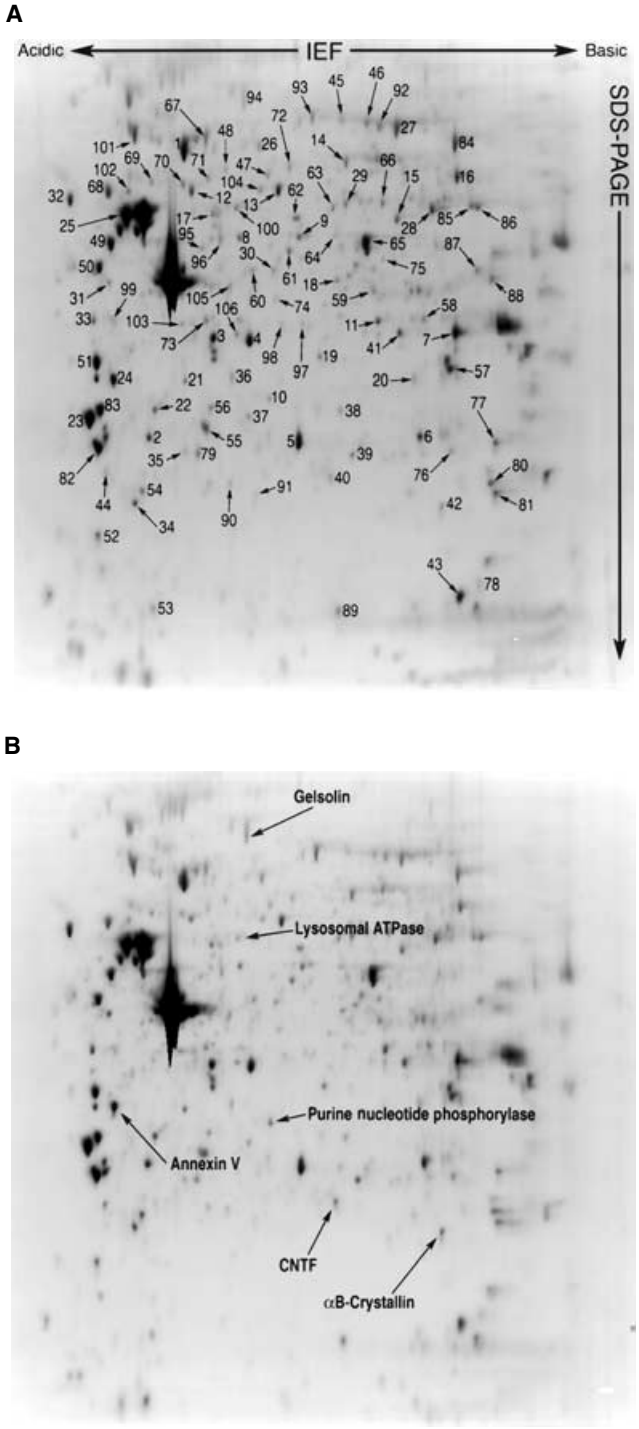

Fig. 2. Representative SYPRO Ruby™ stained two-dimensional-polyacrylamide gel elctrophoresis (PAGE) separations of proteins from dexamethasone- or vehicle-treated cultured podocytes. Protein extracts from podocytes treated for 30 minutes with vehicle alone (*A*) or with 1 μmol/L dexamethasone (*B*) and cultured in fresh medium for 3 days were separated by two-dimensional-PAGE and the resulting gels stained with SYPRO Ruby™. Positions of protein spots identified by matrix-assisted laser desorption time-of-flight (MALDI-TOF) mass spectroscopy and peptide fingerprinting are shown (A), and positions of proteins differentially regulated by dexamethasone are indicated separately (B).

common in cultured cell proteomes were members of the annexin family, heat shock proteins, and actin cytoskeletal proteins.

We identified six proteins whose expression was altered by dexamethasone treatment. Of these proteins, the lysosomal ATP-driven proton pump was the only protein significantly decreased by dexamethasone-treatment. The lysosomal proton pump is responsible for maintaining the acidic conditions required for activity of hydrolytic enzymes present in this organelle, and is a member of a large family of proteins responsible for proton transport across a number of eukaryotic membranes. A recent study in cultured podocytes (in a different line than those used in the current study) has shown that interleukin (IL)-4 and IL-13, lymphocytic cytokines that may be implicated in induction of nephrotic syndrome, can stimulate proton flux across the basolateral membrane of these cells, presumably by increasing the basolateral fusion of lysosomal or endosomal vesicles [41]. This process may lead to changes in intracellular trafficking and to increased proteolytic activity at the basolateral membrane of podocytes, suggesting that the lysosomal ATPase (or another proton pump) may play a role in the development of changes in podocyte foot process morphology characteristic of nephrotic syndrome by enhancing the degradation of transmembrane receptors in podocytes or extracellular matrix proteins. Furthermore, our observed down-regulation of this enzyme in cultured podocytes in response to dexamethasone suggests the hypothesis that down-regulation of lysosomal ATPase may act to protect the podocyte from injury.

The amount of three proteins, the IL-6–type cytokine, CNTF, and two small heat shock proteins, αB-crystallin and hsp27, increased significantly in podocytes 3 days after dexamethasone treatment as determined by Western blotting. CNTF was first isolated as a factor necessary for the survival of chick embryo ciliary ganglionic neurons [42], and has subsequently been shown to enhance survival and protect a variety of different cells from injury [43]. CNTF is found in a variety of tissues, and high expression levels have been measured in the kidney [44]. Both αB-crystallin and the closely related hsp27 are widely expressed proteins that may interact with both actin and intermediate filaments [45–48], act as molecular chaperones [49, 50], and can induce thermotolerance [51, 52]. αB-crystallin has previously been shown to be induced in NIH-3T3 cells by treatment with dexamethasone, and the increase in αB-crystallin correlated with an increase in thermoprotection [53]. The time course of enhanced αB-crystallin expression after treatment in this study was similar to the results we observed in cultured podocytes. In a separate study, comparative two-dimensional-PAGE revealed that αB-crystallin was the protein whose expression was most altered by dexamethasone in NIH-3T3 cells [54]. However, the expression

Table 2. Proteins altered by dexamethasone

Protein	Density (control)	Density (dexamethasone)	% Change[a]	*P* value
ATPase, H+ transport, lysosomal	25355 ± 6831	18322 ± 4066	−72	0.030
Annexin 5	128013 ± 47339	192253 ± 37242	150	0.026
Ciliary neurotrophic factor	31776 ± 9584	62590 ± 9762	197	0.000
αB-Crystallin	51925 ± 17872	85423 ± 23515	165	0.020
Gelsolin	47927 ± 26249	79477 ± 34044	166	0.062
Purine nucleotide phosphorylase	30662 ± 5984	65267 ± 8235	213	0.000

[a]Percentage change in mean dexamethasone density compared to mean control density ($N = 7$); mean normalized density ± SD.

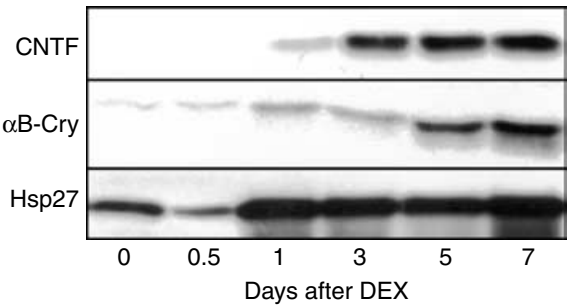

Fig. 3. Representative Western blots of protein extracts of podocytes at various times after dexamethasone treatment. Proteins were extracted from podocytes at 0, 0.5, 1, 3, 5, or 7 days after treatment for 30 minutes with 1 μmol/L dexamethasone and subjected to Western blotting using antibodies against ciliary neurotophic factor (CNTF), αB-crystallin, or heat shock protein 27 (hsp27) as indicated at left. After application of secondary antibodies and chemiluminescent visualization, determination of absolute amounts of protein were made by comparison of luminescence intensities to those of serial dilutions of specific standard proteins separated in the same gels, and comparisons were made to time-matched control values (see text for results).

of hsp27 was not shown to be altered by dexamethasone in NIH-3T3 cells [53], though in rat cerebellar slices given a mild heat shock after treatment with the glucocorticoid corticosterone, hsp27 was induced compared to tissue receiving heat shock alone [55], the expression of hsp27 was induced by dexamethasone in osteoblasts [56] and mouse skin [57], and the expression of both hsp27 and αB-crystallin were induced by dexamethasone in muscle cells [58]. Recent studies have suggested protective or ameliorative roles for these proteins in the kidney, describing enhanced expression of CNTF and CNTFRα in injured kidney tissues following ischemia/reperfusion injury [59], and that the expression of hsp27 is directly related to the resistance of cultured podocytes to the morphologic and actin cytoskeletal injury caused by the podocyte toxin, PAN [24].

The amounts of gelsolin, annexin V, and purine nucleoside phosphorylase increased significantly in podocytes 3 days after dexamethasone treatment as determined by comparisons of two-dimensional-PAGE separations. Gelsolin is the most potent known actin filament-severing protein, and the only known calcium-dependent actin-severing protein. Gelsolin has only been detected in the podocyte during fetal development [60]. A gelsolin mutation resulting in a single aspartate to asparagine substitution at amino acid 187 results in Finnish-type familial amyloidosis with severe neural effects [61], but individuals with homozygous mutations at this locus also suffer severe renal disease [62]. These results, coupled with the increasing body of evidence linking proteins critical to podocyte function to the actin cytoskeleton [63–66], suggest that altering gelsolin levels in the tightly regulated system controlling actin polymerization may have profound effects on podocyte function. Annexins are highly conserved calcium-binding proteins, and after calcium binding annexin V binds with high affinity to anionic phospholipids [67]. Annexin V has been localized to the podocyte in vivo, and the amount of annexin V excreted in the urine increased with increasing renal injury in experimental rat glomerulonephritis [68]. However, the up-regulation of annexin V we discovered in cultured podocytes in response to dexamethasone may be consequence of their differentiation. Glucocorticoids have previously been demonstrated to induce differentiation in a variety of cells in culture [69], and proteomic analyses of cultured cells have found annexin V in quiescent cultures of primary human umbilical vein endothelial cells, and down-regulated in adaptation of bladder carcinoma cells to culture [39, 70]. Purine nucleoside phosphorylase catalyzes the phosphorolysis of the N-ribosidic bonds of purine nucleosides and deoxynucleosides, and is a key enzyme in the purine salvage pathway. A variety of mutations in the gene encoding purine nucleoside phosphorylase result in the rare autosomal-recessive disease, purine nucleoside phosphorylase deficiency, that results primarily in neural and T-cell defects [71]. However, no renal abnormalities were observed in either human patients with purine nucleoside phosphorylase deficiency or in purine nucleoside phosphorylase knockout mice, suggesting that purine nucleoside phosphorylase is not essential for podocyte function.

CONCLUSION

We have performed an initial analysis of the proteome of cultured, differentiated podocytes, and have identified six proteins whose expression is altered in these cells

by treatment with dexamethasone. The up-regulation of CNTF and αB-crystallin was confirmed by quantitative Western blotting, and hsp27, a protein closely related to αB-crystallin, was also found to be upregulated in podocytes by dexamethasone treatment. All three of these proteins have previously been shown to protect cells against cell stress and injury (hsp27 and αB-crystallin) or to enhance cell survival (CNTF), suggesting that the up-regulation of one or more of these proteins may account for the observed protective and ameliorative effects of dexamethasone treatment against podocyte injury. These results demonstrate that dexamethasone acts directly on podocytes leading to increases in the expression of proteins with known protective roles, and suggest potential mechanisms of action for the therapeutic effect of glucocorticoids in diseases such as nephrotic syndrome that primarily affect the glomerular podocyte.

ACKNOWLEDGMENTS

This work was supported in part by NIH grants K08 DK02455-01 and R01 DK55602 to W.E.S., as well as R01 HL66358-01, R21 DK62086-01, the Department of Veterans Affairs Merit Review, and The Commonwealth of Kentucky Research Challenge Trust Fund to J.B.K.

Reprint requests to Richard F. Ransom, Ph.D., Pediatric Nephrology Division, University of Michigan, 8220D MSRB III, 1150 W. Medical Center Dr. Ann Arbor, MI 48109–0646.
E-mail: rransom@umich.edu

REFERENCES

1. Kriz W: Evolving role of the podocyte in chronic renal failure. *Kidney Blood Press Res* 20:180–183, 1997
2. Kriz W: Podocyte is the major culprit accounting for the progression of chronic renal disease. *Microsc Res Tech* 57:189–195, 2002
3. Antignac C: Genetic models: Clues for understanding the pathogenesis of idiopathic nephrotic syndrome. *J Clin Invest* 109:447–449, 2002
4. Coers W, Reivinen J, Miettinen A, *et al*: Characterization of a rat glomerular visceral epithelial cell line. *Exp Nephrol* 4:184–192, 1996
5. Mentzel S, Van Son JP, De Jong AS, *et al*: Mouse glomerular epithelial cells in culture with features of podocytes in vivo express aminopeptidase A and angiotensinogen but not other components of the renin-angiotensin system. *J Am Soc Nephrol* 8:706–719, 1997
6. Ardaillou N, Lelongt B, Turner N, *et al*: Characterization of a simian virus 40-transformed human podocyte cell line producing type IV collagen and exhibiting polarized response to atrial natriuretic peptide. *J Cell Physiol* 152:599–616, 1992
7. Saleem MA, O'Hare MJ, Reiser J, *et al*: A conditionally immortalized human podocyte cell line demonstrating nephrin and podocin expression. *J Am Soc Nephrol* 13:630–638, 2002
8. Mundel P, Reiser J, Zuniga Mejia Borja A, *et al*: Rearrangements of the cytoskeleton and cell contacts induce process formation during differentiation of conditionally immortalized mouse podocyte cell lines. *Exp Cell Res* 236:248–258, 1997
9. Mundel P, Heid HW, Mundel TM, *et al*: Synaptopodin: An actin-associated protein in telencephalic dendrites and renal podocytes. *J Cell Biol* 139:193–204, 1997
10. Hoyer JR: Idiopathic nephrotic syndrome with minimal changes. *Contemp Issues Nephrol* 9:145–170, 1982
11. Vernier RL, Papermaster BW, Good RA: Aminonucleoside nephrosis. I. Electron microscopic study of the renal lesion in rats. *J Exp Med* 109:115–126, 1958
12. Ryan GP, Karnovsky MJ: An ultrastructural study of the mechanisms of proteinuria in aminonucleoside nephrosis. *Kidney Int* 8:219–232, 1975
13. Ito K, Ger YC, Kawamura S: Actin filament alterations in glomerular epithelial cells of adriamycin-induced nephrotic rats. *Acta Pathol Jpn* 36:253–260, 1986
14. Caulfield JP, Reid JJ, Farquhar MG: Alterations of the glomerular epithelium in acute aminonucleoside nephrosis. Evidence for formation of occluding junctions and epithelial cell detachment. *Lab Invest* 34:43–59, 1976
15. Farquhar MG, Vernier RL, Good RA: An electron microscopic study of the glomerulus in nephrosis, glomerulonephritis and lupus erythematosus. *J Exp Med* 106:649–660, 1957
16. Whiteside C, Prutis K, Cameron R, Thompson J: Glomerular epithelial detachment, not reduced charge density, correlates with proteinuria in adriamycin and puromycin nephrosis. *Lab Invest* 61:650–660, 1989
17. Barratt TM, Clark G: Minimal change nephrotic syndrome and focal segmental glomeruluosclerosis, in *Pediatric Nephrology*, 3rd ed., edited by Holliday MA, Barratt TM, Avner ED, Baltimore, Williams & Wilkins, 1994, pp 767–787
18. Tanaka R, Yoshikawa N, Nakamura H, Ito H: Infusion of peripheral blood mononuclear cell products from nephrotic children increases albuminuria in rats. *Nephron* 60:35–41, 1992
19. Yoshizawa N, Kusumi Y, Matsumoto K, *et al*: Studies of glomerular permeability factor in patients with minimal-change nephrotic syndrome. *Nephron* 51:370–376, 1989
20. Garin EH: Circulating mediators of proteinuria in idiopathic minimal lesion nephrotic syndrome. *Pediatr Nephrol* 14:872–878, 2000
21. Shalhoub RJ: Pathogenesis of lipoid nephrosis: A disorder of T-cell function. *Lancet* 2:556–560, 1974
22. Yan K, Kudo A, Hirano H, *et al*: Subcellular localization of glucocorticoid receptor protein in the human kidney glomerulus. *Kidney Int* 56:65–73, 1999
23. Ransom RF, Li Y, Lam N, Smoyer WE: Glucocorticoids stabilize podocyte microfilaments and protect and enhance recovery from PAN-induced injury. *J Am Soc Nephrol* 13:526A, 2002
24. Smoyer WE, Ransom RF: Hsp27 regulates podocyte cytoskeletal changes in an in vitro model of podocyte process retraction. *FASEB J* 16:315–326, 2002
25. Thongbookerd V, Luengpailin J, Cao J, *et al*: Fluoride exposure attenuates expression of streptococcus pyrogenes virulence factors. *J Biol Chem* 277:16599–16605, 2002
26. Clarke W, Silverman BC, Zhang Z, *et al*: Characterization of renal allograft rejection by urinary proteomic analysis. *Ann Surg* 237:660–664, 2003
27. Cutler P, Bell DJ, Birrell HC, *et al*: An integrated proteomic approach to studying glomerular nephrotoxicity. *Electrophoresis* 20:3647–3658, 1999
28. Thongboonkerd V, Klein JB, Pierce WM, *et al*: Sodium loading changes urinary protein excretion: a proteomic analysis. *Am J Physiol Renal Physiol* 284:F1155–F1163, 2003
29. Thongboonkerd V, McLeish KR, Arthur JM, Klein JB: Proteomic analysis of normal human urinary proteins isolated by acetone precipitation or ultracentrifugation. *Kidney Int* 62:1461–1469, 2002
30. Unwin RD, Craven RA, Harnden P, *et al*: Proteomic changes in renal cancer and co-ordinate demonstration of both the glycolytic and mitochondrial aspects of the Warburg effect. *Proteomics* 3:1620–1632, 2003
31. Unwin RD, Harnden P, Pappin D, *et al*: Serological and proteomic evaluation of antibody responses in the identification of tumor antigens in renal cell carcinoma. *Proteomics* 3:45–55, 2003
32. Cheung PY, Lai WP, Lau HY, *et al*: Acute and chronic effect of dietary phosphorus restriction on protein expression in young rat renal proximal tubules. *Proteomics* 2:1211–1219, 2002
33. Arthur JM, Thongboonkerd V, Scherzer JA, *et al*: Differential expression of proteins in renal cortex and medulla: a proteomic approach. *Kidney Int* 62:1314–1321, 2002
34. Waghray A, Feroze F, Schober MS, *et al*: Identification of androgen-regulated genes in the prostate cancer cell line LNCaP by serial analysis of gene expression and proteomic analysis. *Proteomics* 1:1327–1338, 2001
35. Thongboonkerd V, Gozal E, Sachleben LR, Jr., *et al*: Proteomic analysis reveals alterations in the renal kallikrein pathway during hypoxia-induced hypertension. *J Biol Chem* 277:34708–34716, 2002

36. Charlwood J, Skehel JM, King N, *et al*: Proteomic analysis of rat kidney cortex following treatment with gentamicin. *J Proteome Res* 1:73–82, 2002
37. Witzmann FA, Fultz CD, Grant RA, *et al*: Differential expression of cytosolic proteins in the rat kidney cortex and medulla: Preliminary proteomics. *Electrophoresis* 19:2491–2497, 1998
38. Boraldi F, Bini L, Liberatori S, *et al*: Normal human dermal fibroblasts: Proteomic analysis of cell layer and culture medium. *Electrophoresis* 24:1292–1310, 2003
39. Bruneel A, Labas V, Mailloux A, *et al*: Proteomic study of human umbilical vein endothelial cells in culture. *Proteomics* 3:714–723, 2003
40. Desrivieres S, Prinz T, Castro-Palomino Laria N, *et al*: Comparative proteomic analysis of proliferating and functionally differentiated mammary epithelial cells. *Mol Cell Proteomics* 28:28, 2003
41. Van Den Berg JG, Aten J, Annink C, *et al*: Interleukin-4 and -13 promote basolateral secretion of H(+) and cathepsin L by glomerular epithelial cells. *Am J Physiol Renal Physiol* 282:F26–F33, 2002
42. Barbin G, Manthorpe M, Varon S: Purification of the chick eye ciliary neuronotrophic factor. *J Neurochem* 43:1468–1478, 1984
43. Regulier E, Pereira de Almeida L, Sommer B, *et al*: Dose-dependent neuroprotective effect of ciliary neurotrophic factor delivered via tetracycline-regulated lentiviral vectors in the quinolinic acid rat model of Huntington's disease. *Hum Gene Ther* 13:1981–1990, 2002
44. Ebendal T: Comparative screening for ciliary neurotrophic activity in organs of the rat and chicken. *J Neurosci Res* 17:19–24, 1987
45. Bennardini F, Wrzosek A, Chiesi M: αB-crystallin in cardiac tissue: Association with actin and desmin filaments. *Circ Res* 71:288–294, 1992
46. Djabali K, Piron G, de Nechaud B, Portier MM: alphaB-crystallin interacts with cytoplasmic intermediate filament bundles during mitosis. *Exp Cell Res* 253:649–662, 1999
47. Benndorf R, Hayess K, Ryazantsev S, *et al*: Phosphorylation and supramolecular organization of murine small heat shock protein HSP25 abolish its actin polymerization-inhibiting activity. *J Biol Chem* 269:20780–20784, 1994
48. Perng MD, Cairns L, vanden IP, *et al*: Intermediate filament interactions can be altered by HSP27 and alphaB-crystallin. *J Cell Sci* 112:2099–2112, 1999
49. Horwitz J: α-Crystallin can function as a molecular chaperone. *Proc Natl Acad Sci USA* 89:10449–10453, 1992
50. Rogalla T, Ehrnsperger M, Preville X, *et al*: Regulation of hsp27 oligomerization, chaperone function, and protective activity against oxidative stress/tumor necrosis factor α by phosphorylation. *J Biol Chem* 274:18947–18956, 1999
51. Aoyama A, Frohli E, Schafer R, Klemenz R: αB-crystallin expression in mouse NIH 3T3 fibroblasts: Glucocorticoid responsiveness and involvement in thermal protection. *Mol Cell Biol* 13:1824–1835, 1993
52. Landry J, Chretien P, Lambert H, *et al*: Heat shock resistance conferred by expression of the human HSP27 gene in rodent cells. *J Cell Biol* 109:7–15, 1989
53. Aoyama A, Frohli E, Schafer R, Klemenz R: Alpha B-crystallin expression in mouse NIH 3T3 fibroblasts: glucocorticoid responsiveness and involvement in thermal protection. *Mol Cell Biol* 13:1824–1835, 1993
54. Scheier B, Foletti A, Stark G, *et al*: Glucocorticoids regulate the expression of the stressprotein αB-crystallin. *Mol Cell Endocrinol* 123:187–198, 1996
55. Barr CS, Dokas LA: Glucocorticoids regulate the synthesis of HSP27 in rat brain slices. *Brain Res* 847:9–17, 1999
56. Kozawa O, Niwa M, Hatakeyama D, *et al*: Specific induction of heat shock protein 27 by glucocorticoid in osteoblasts. *J Cell Biochem* 86:357–364, 2002
57. Tuckermann JP, Reichardt HM, Arribas R, *et al*: The DNA binding-independent function of the glucocorticoid receptor mediates repression of AP-1-dependent genes in skin. *J Cell Biol* 147:1365–1370, 1999
58. Nedellec P, Edling Y, Perret E, *et al*: Glucocorticoid treatment induces expression of small heat shock proteins in human satellite cell populations: Consequences for a desmin-related myopathy involving the R120G alpha B-crystallin mutation. *Neuromuscul Disord* 12:457–465, 2002
59. Yang CW, Lim SW, Han KW, *et al*: Upregulation of ciliary neurotrophic factor (CNTF) and CNTF receptor alpha in rat kidney with ischemia-reperfusion injury. *J Am Soc Nephrol* 12:749–757, 2001
60. Lueck A, Brown D, Kwiatkowski DJ: The actin-binding proteins adseverin and gelsolin are both highly expressed but differentially localized in kidney and intestine. *J Cell Sci* 111:3633–3643, 1998
61. Maury CP: Gelsolin-related amyloidosis. Identification of the amyloid protein in Finnish hereditary amyloidosis as a fragment of variant gelsolin. *J Clin Invest* 87:1195–1199, 1991
62. Maury CP, Kere J, Tolvanen R, de la Chapelle A: Homozygosity for the Asn187 gelsolin mutation in Finnish-type familial amyloidosis is associated with severe renal disease. *Genomics* 13:902–903, 1992
63. Doublier S, Ruotsalainen V, Salvidio G, *et al*: Nephrin redistribution on podocytes is a potential mechanism for proteinuria in patients with primary acquired nephrotic syndrome. *Am J Pathol* 158:1723–1731, 2001
64. Smoyer WE, Mundel P, Gupta A, Welsh MJ: Podocyte α-actinin induction precedes foot process effacement in experimental nephrotic syndrome. *Am J Physiol* 273:F150–F157, 1997
65. Lehtonen S, Zhao F, Lehtonen E: CD2-associated protein directly interacts with the actin cytoskeleton. *Am J Physiol Renal Physiol* 283:F734–F743, 2002
66. Sellin L, Huber TB, Gerke P, *et al*: NEPH1 defines a novel family of podocin interacting proteins. *FASEB J* 17:115–117, 2003
67. Reutelingsperger CP, van Heerde WL: Annexin V, the regulator of phosphatidylserine-catalyzed inflammation and coagulation during apoptosis. *Cell Mol Life Sci* 53:527–532, 1997
68. Matsuda R, Kaneko N, Horikawa Y, *et al*: Localization of annexin V in rat normal kidney and experimental glomerulonephritis. *Res Exp Med (Berlin)* 200:77–92, 2001
69. Kawashima H, Ogose A, Hayami T, *et al*: Effect of dexamethasone on growth inhibition and chondrogenic maturation of human chondrosarcoma. *J Orthop Sci* 8:341–345, 2003
70. Celis A, Rasmussen HH, Celis P, *et al*: Short-term culturing of low-grade superficial bladder transitional cell carcinomas leads to changes in the expression levels of several proteins involved in key cellular activities. *Electrophoresis* 20:355–361, 1999
71. Markert ML: Purine nucleoside phosphorylase deficiency. *Immunodefic Rev* 3:45–81, 1991